Synthetically Generated Turbulent Boundary-Layer Development and Structure

F. W. Chambers*
Lockheed-Georgia Company, Marietta, Georgia

Experiments were conducted to investigate the turbulent boundary-layer skin-friction drag reductions that could be attained through the creation of boundary layers with controlled spatial and temporal scales. The goals of the experiments were to determine the magnitude of any drag reductions and to illuminate the turbulent structure of the flow. Measurements of mean and fluctuating velocities were performed, providing mean velocity profiles, turbulence intensity profiles, bursting frequency, VITA conditionally averaged velocity, and ensemble phase-averaged velocity in the synthetically generated turbulent boundary layer and a reference turbulent flow produced with a two-dimensional trip. Significant drag reductions were not found as the changes in the flow appeared to be of the form of shifts in the effective origin of the boundary-layer development. However, the outer flow in the synthetic boundary layer was altered, maintaining some of the periodicity of the generation.

Nomenclature

f = boundary-layer bursting frequency
f^+ = $f\nu/u^{*2}$ = inner scaled bursting frequency
t = time
t^+ = tu^{*2}/ν = inner scaled time
U = local mean velocity
U_0 = freestream velocity
u' = rms turbulent velocity fluctuation
u^+ = U/u^* = inner scaled mean velocity
$\langle u \rangle$ = conditionally averaged velocity
$\tilde{u}$ = phase-averaged velocity
u^* = $[\tau_w/\rho]^{1/2}$ = wall friction velocity
x = coordinate in streamwise direction
y = coordinate normal to the wall
y^+ = yu^*/ν = inner scaled coordinate normal to the wall
δ = boundary-layer thickness
θ = $\int_0^\infty \frac{U}{U_0}\left(1-\frac{U}{U_0}\right)dy$ = boundary-layer momentum thickness
ν = fluid kinematic viscosity
ρ = fluid mass density
τ_w = wall shear stress

Introduction

SYNTHETICALLY generated turbulent boundary layers have been studied previously by Coles and Barker[1] and Coles and Savas.[2] The flows were developed by artificially producing arrays of turbulent spots in initially laminar boundary layers. Coles and Savas identified generating parameter ranges in which the spots or large eddies maintained structural coherence for relatively large downstream distances. Savas and Coles[3] have recently described this work in more detail. The importance of the large scales in boundary-layer behavior is well known. This demonstrated ability to generate controlled large scales suggested to Thomas[4] that skin-friction drag reductions might be attained in the synthetic boundary layers. The measurements of Coles and Barker and Coles and Savas had not provided information on the skin friction of the boundary layers.

Presented as Paper 85-0534 at the AIAA Shear Flow Control Conference, Boulder, CO, March 12-14, 1985; received May 2, 1985; revision received April 1, 1986.

*Scientist, Advanced Research Organization. Member AIAA.

Experiments were initiated at Lockheed[5] and at NASA Langley[6] to investigate the drag reduction possibilities of these boundary layers. The synthetic boundary layer in the Lockheed experiment was formed with a minimum spanwise spot spacing of approximately four local boundary-layer thicknesses and with relatively low-frequency spot generation. This experiment indicated that alterations in the boundary-layer structure could be produced that were observable far downstream. Changes in the local skin-friction coefficient were also observed, suggesting that the technique did have a skin-friction reduction potential. However, the experiment was limited to X-Reynolds numbers of 7.5×10^5 and the difference between alterations in the boundary-layer development and simple shifts in the origins of the development were difficult to isolate.

Goodman[6] at NASA Langley conducted a similar experiment employing acoustic drivers to generate spots with a spanwise spacing of approximately one local boundary-layer thickness. The acoustic excitation allowed generation at much higher frequencies. Skin friction was measured using an air-bearing wall drag balance. The results indicated that local skin-friction reductions of as much as 15% could be obtained within approximately 120 boundary-layer thicknesses of the spot generators. Smoke flow visualization and pitot probe velocity profile surveys also were employed, but detailed measurements of the turbulent structure of the boundary layers were not reported. The maximum X-Reynolds number was limited to approximately 5.6×10^5.

The present work was planned to extend the earlier effort to higher Reynolds numbers and was aimed at determining the downstream extent of alterations in skin friction and turbulence and the role of shifts in the effective origin of development of the flows. It was desired to increase the range of generation parameters investigated, to perform measurements farther downstream of the transition region, and to clarify whether the temporal and spatial scales of the generation were maintained for long distances downstream. To attain these goals, the flat-plate test assembly was lengthened and additional spot generator holes were added. A series of hot-wire anemometer measurements were performed providing mean velocity profiles, turbulence intensity profiles, and phase- and conditionally-averaged velocities.

Apparatus and Instrumentation

Boundary layers were developed on a smooth flat plate in a closed-return, low-turbulence wind tunnel. The freestream

velocity was approximately 8.7 m/s and the turbulence intensity was less than 0.04%. The tunnel test section was nominally $0.6 \times 0.9 \times 6$ m. The cross section was enlarged with downstream distance to maintain a zero pressure gradient. The smooth flat plate was 0.9 m wide and 5.0 m long. It had a tapered, rounded leading edge and a trailing-edge flap to control the leading-edge stagnation point. Sidewall contamination of the boundary layer was reduced by venting corner flow to the low-pressure region behind the plate through slots.

The synthetic boundary layer was formed by periodically blowing arrays of small air jets into the bottom of the laminar boundary layer 0.3 m downstream of the leading edge as shown in Fig. 1. The jets generated arrays of transitional turbulent spots that, in turn, interacted to form the turbulent boundary layers. The jets were discharged from a transverse row of 82 holes 1 mm in diameter spaced 10 mm apart. The pulsed jets were produced from a compressed air supply using solenoid valves. The jets were operated with a duration of 10 ms and a maximum velocity of approximately 5 m/s. These conditions had earlier been found to produce good turbulent spots, as shown in Fig. 2 and described in more detail by Chambers and Thomas.[7] The repeatability of the pulses is illustrated in Fig. 3 by the velocity-time record of the flow on the centerline of one jet. The velocity was measured with a hot-wire anemometer probe centered above the jet. In order to fire one-half of the jets at a time, alternate holes were connected to separate manifolds. Individual solenoid valves fed the two manifolds, allowing variable phase between firings of the two sets of jets. The boundary layer at the jet location was laminar with an X-Reynolds number equal to 1.7×10^5 and a thickness of 4.0 mm. A tripped turbulent boundary layer was used as a reference case. It was formed with a two-dimensional 3 mm diam trip rod mounted 0.3 m from the leading edge, the same location as the jets. This trip was chosen for ease of mounting and dismounting and for repeatable performance. It was sized to produce fully turbulent flow rapidly. Boundary-layer measurements were performed at X-Reynolds numbers between approximately 5.0×10^5 and 25.0×10^5.

Velocity measurements were performed using DISA 55M10 CTA constant-temperature anemometers with DISA 55P15 miniature hot-wire boundary-layer probes. The probes were constructed of 5 μm diam wire with a 1.25 mm sensor length and were operated at an overheat ratio of 1.8. Calibration was performed in the freestream against a pitot static tube and a pressure transducer. A modified King's law was fit to the calibration points with a velocity exponent $n = 0.45$.

The probes were mounted on a computer-controlled three-dimensional traversing system using stepping motor drives. It was capable of repeatably positioning the probe at a minimum height of 0.13 mm above the plate and traversing it outward to a maximum height of 94 mm.

Anemometer dc and ac voltages, pressure transducer output voltage, and spot-generating solenoid valve driving voltage were acquired and digitized on a high-speed data acquisition system controlled through a VAX 11/730 computer. Measurements of mean velocity profiles alone were acquired using a sampling rate of 2 kHz and a record length of 8.192 s. Measurements incorporating turbulence parameters were acquired at 8 kHz with a record length of 8.192 s.

Mean velocity profiles were measured with the hot wire anemometer at 39 points across the boundary layer. The lowest 12 points of each profile were evenly spaced between y^+ equal to 5 and 200. The remaining points were evenly spaced to a height of approximately 1.2 times the mean boundary layer thickness. A final point was positioned well out in the freestream.

The boundary-layer displacement and momentum thicknesses were calculated by numerically integrating the measured velocity profiles. The bottom of the profile was extrapolated to zero at the wall and the points at velocities greater than 99.5% of the nominal freestream velocity were smoothed.

Estimates of the local skin-friction coefficient were made with the boundary-layer momentum integral equation and fits of the measured velocity profiles to the log law of the wall. The momentum integral equation was preferred in principle, for it assumes only two-dimensionality. However, in practice, the local skin-friction coefficients are determined from the derivative of a curve fit to the measured momentum thicknesses. The curve fit is problematic and it is felt that the trends are observed better by simply considering the momentum thickness distributions.

The fits of the velocity profile to the log law of the wall amounted to an automated Clauser chart using the profile points lying between y^+ equal to 50 and 200. The standard log law coefficients ($A = 2.44$ and $B = 5.0$) were found to represent the synthetic boundary-layer profiles well in the ranges studied. The estimated skin-friction coefficient was that for which the squared errors in the fit were a minimum.

The anemometer ac voltage was high-pass filtered at 0.07 Hz and amplified before digitization. Turbulent velocity fluctuations about the mean were calculated for the digitized anemometer records by employing the anemometer calibration coefficients and the local mean velocity. True averages over the record were used to calculate the mean square and root mean square velocity fluctuations

Conditional averages and boundary-layer bursting frequencies were determined using the variable-interval time averaging (VITA) technique of Blackwelder and Kaplan.[8] Measurements were performed at $y^+ = 15$ using a threshold of 1.0 and a VITA/averaging time of 10 inner time units. The hot-wire anemometer probe employed had an inner scaled width of no more than 33 wall units. The measured bursting frequencies were corrected for the sensor length using the equation suggested by Blackwelder and Haritonidis.[9]

Ensemble phase averages were formed for the absolute velocities and the velocity fluctuations at locations corresponding to $y^+ = 15$ and $y/\delta = 0.8$. The averages were triggered on the signal used to drive the solenoid valves forming the synthetic boundary layer. The same procedure was used for the

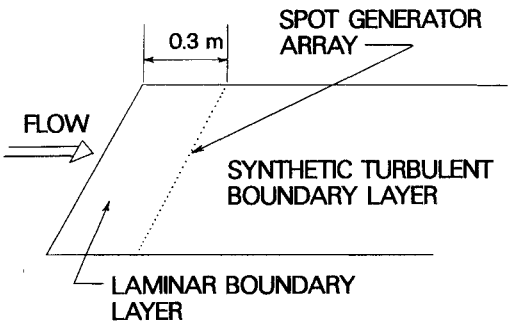

Fig. 1 Experimental configuration.

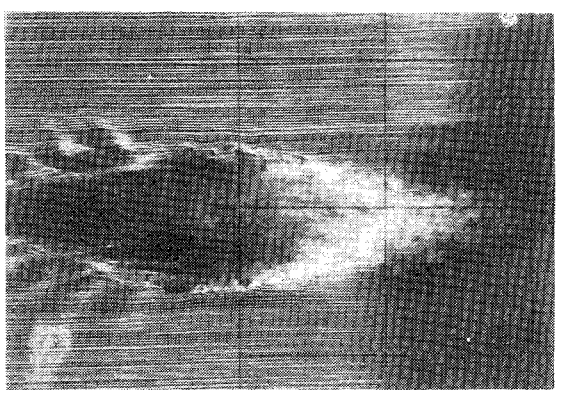

Fig. 2 Typical single turbulent spot.

tripped flows as a check on the validity of the phase averages. In the tripped flow cases, the trigger signal was not connected to anything influencing the flow.

Experimental Results

Measurements were first performed to verify the establishment of a standard nominally zero pressure gradient two-dimensional boundary-layer flow. After a number of iterations adjusting the spread of the walls of the tunnel and the gaps at the edges of the plate, the flow was satisfactory. The static pressure gradient measured through wall taps is shown in Fig. 4. The pressure gradient was nominally zero to within ±3%. Measurements of velocity profiles over the entire span of the plate showed that the gaps at the edges of the plate did reduce corner flow contamination. The central 0.7 m of the 0.9 m wide plate exhibited very good flow uniformity over the entire measurement range, which extended 4.5 m downstream from the plate leading edge.

Mean velocity profiles were measured to assess the development of the synthetically generated turbulent boundary layers in terms of the momentum thickness and the local skin-friction coefficient. Typical mean velocity profiles for the tripped flow and a synthetic boundary layer are shown in dimensionless form in Fig. 5. For the synthetic boundary layers, velocity profile measurements were performed at spanwise positions covering a range of three jet spanwise spacings. No significant spanwise variations were found in these measurements and the rest of the measurements were conducted on the centerline. Fitting these profiles to the log law of the wall by choosing a best fit skin-friction coefficient results in the inner scaled profiles of Fig. 6. The synthetic boundary-layer flows fit the log law profile with standard coefficients very well in most locations. Only at the measurement stations closest to the spot generators did the synthetic profiles exhibit any systematic deviation from the profile. At these locations, it is difficult to resolve whether the synthetic boundary layer has a different wall layer thickness than a naturally turbulent flow or whether the flow simply is transitional and not yet fully turbulent.

A limited study was performed of the effects of the synthetic boundary-layer generation parameters on the boundary-layer development. The frequency of generation, the phase difference between the two manifolds, and the spanwise spacing between adjacent spot generator jets (and hence the number of jets) were varied. Frequencies were 10-30 Hz, phase differences 180, 0, and 90 deg, and spacings 10, 20, and 30 mm. It was desired to discover generation parameters that produced long-term downstream effects upon the structure of the synthetic boundary layers. Consequently, measurements of the synthetic boundary layers were performed at large distances from the generation location. Three velocity profiles were measured for each of the generation parameter cases at distances of 3.00, 3.35, and 3.70 m downstream of the spot generators. The momentum thickness distributions and local skin-friction coefficients resulting from these profile measurements are presented in Figs. 7 and 8. Comparisons were made to the tripped flow. It should be observed that this tripped flow exhibits excellent agreement with data for natural turbulent flows and hence serves as an appropriate standard of comparison for the synthetic flows. The comparisons of the measurements do not reveal dramatic changes in the synthetic boundary-layer behavior. The momentum thickness magnitudes, the slopes of the momentum thickness distributions and the skin-friction coefficients are quite similar. The small differences may be attributed to scatter in the data, shifts in the origin of development, and changes in the development process. The roughly equal slopes suggest that the largest factor was upstream changes resulting in effective shifts in origin. Thus, within the generation parameter range investigated, no strong influence upon the downstream boundary-layer characteristics was discovered.

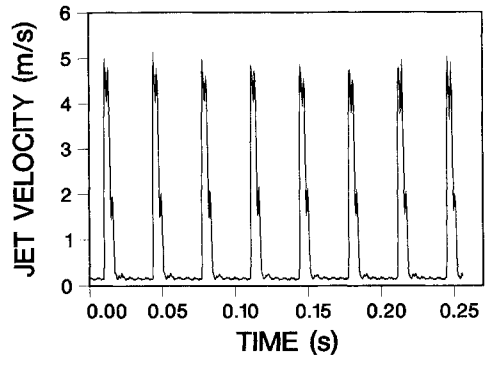

Fig. 3 Spot-generator jet time history.

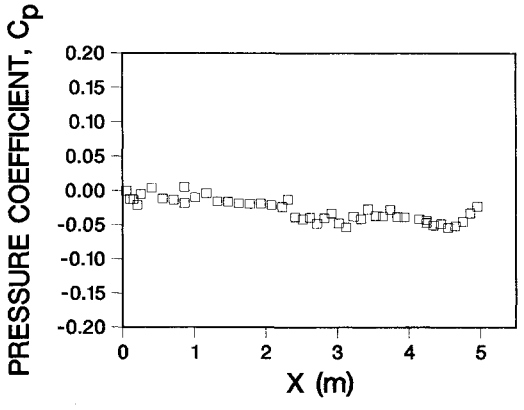

Fig. 4 Pressure distribution along the plate.

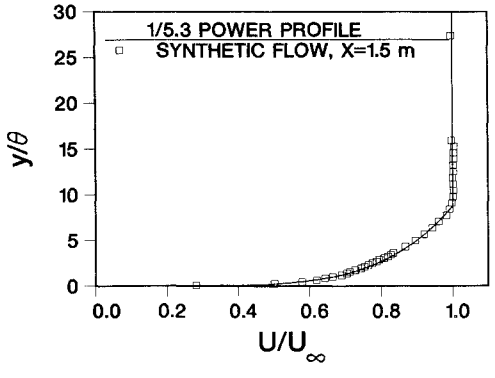

Fig. 5 Dimensionless mean velocity profiles.

In order to determine the nature and extent of the differences between synthetically generated turbulent boundary layers and normal turbulent boundary layers, one synthetic flow and the tripped flow were studied in detail. The synthetic flow was generated with a 10 Hz pulse frequency, a 180 deg phase difference between the two manifolds, and a 10 mm spanwise spacing between jets. Note that, with the 180 deg phase difference, the spacing between jets fired simultaneously was 20 mm. Mean velocity profiles for the synthetic and tripped flows were measured at more than 40 stations ranging between 0.9 and 4.3 m from the plate leading edge.

The mean velocity profiles of the synthetic flow display similarity when scaled with momentum thickness and when scaled with inner variables. The profiles are indistinguishable from those of the tripped flow. However, the momentum thicknesses of the synthetic boundary layer are thinner than those of the tripped flow. The skin-friction coefficients inferred from fits to the law of the wall are higher than those for the tripped flow at the same position.

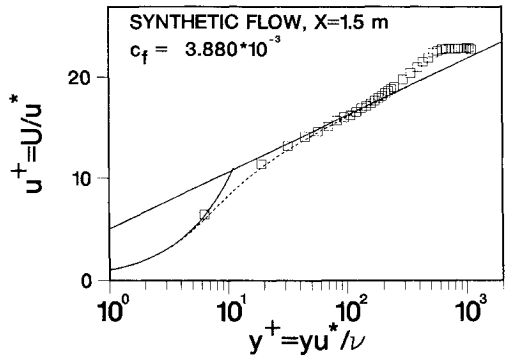

Fig. 6 Inner scaled mean velocity profiles.

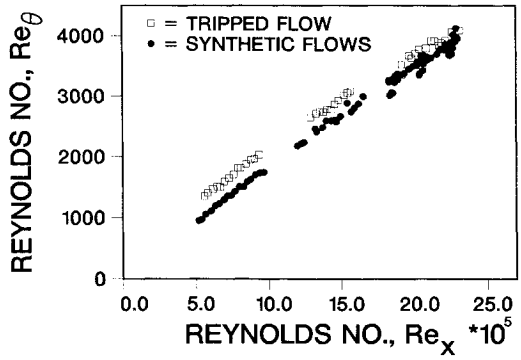

Fig. 7 Momentum thickness variation with generation parameters.

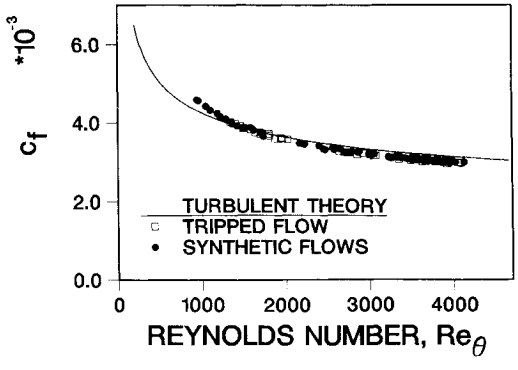

Fig. 8 Skin-friction coefficient variation with generation parameters.

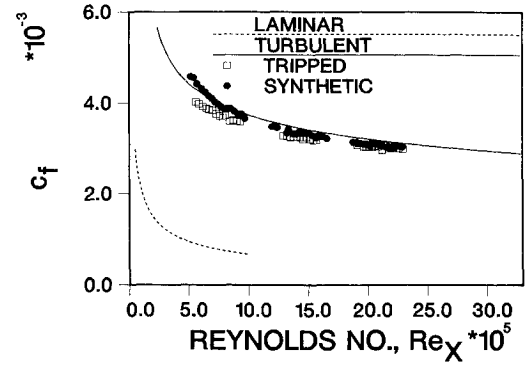

Fig. 9 Skin-friction coefficient as a function of X-Reynolds number.

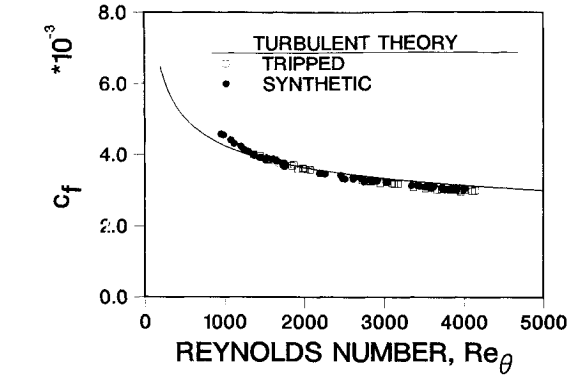

Fig. 10 Skin-friction coefficient as a function of momentum thickness Reynolds number.

The skin-friction coefficients for the two flows are presented as functions of X-Reynolds number in Fig. 9. The figure suggests that the apparent origin of development of the tripped flow is farther upstream than that of the synthetic flow. Replotting the skin-friction coefficients as functions of momentum thickness Reynolds number in Fig. 10 reveals that both cases fall upon the same development curve. Since the skin-friction coefficient is proportional to the streamwise derivative of the momentum thickness for a zero pressure gradient boundary layer, this result implies that the growth of the mean boundary-layer characteristics of the two cases is the same. Thus, the net skin-friction drag differences between the two cases must result solely from differences in the transition region. This particular synthetic boundary layer then appears to develop in the same way as a normal turbulent boundary layer; the controlled temporal and spatial scales used to generate the boundary layer have not had a significant effect upon the mean flow development.

Differences in the turbulence in the two flows were evaluated first by performing measurements of turbulence intensity profiles 1.0, 1.7, 2.3, 2.7, 3.3, and 4.0 m from the leading edge of the plate. Typical profiles for the two cases are shown in Fig. 11. The tripped flow case displays excellent agreement with the characteristics expected for developed turbulent boundary layers. The profiles of the two cases are very much the same and this similarity also holds when the profiles are scaled with momentum thicknesses. Thus, both the mean velocity and the turbulence intensity profiles of the two boundary layers appear very similar at sufficient distances downstream of the trip or the spot generators.

Further investigations of the structure of the synthetic and tripped turbulent boundary-layer flows were conducted using time histories to form conditional averages and ensemble phase averages. Hot-wire anemometers were used to acquire long time records of the flow velocities at $y^+ = 15$, at $y/\delta = 0.8$, and in the freestream. These records were obtained at the streamwise locations previously used for the turbulence intensity profile measurements. The anemometer voltage records were acquired and converted to velocity and the velocity-time records then were stored on disk so that the different averaging techniques could be applied to identical sample records.

The boundary-layer bursting frequency and conditionally averaged velocity at $y^+ = 15$ were calculated using the VITA technique. The bursting frequencies for the two cases are presented in Fig. 12 as functions of X-Reynolds number. It may be observed that the detected bursting frequencies are in fairly good agreement with each other except at the earliest measuring stations. The bursting frequencies are also in good agreement with values in the literature. Note that the detected bursting frequencies are approximately three times the frequency used to produce the synthetic turbulent boundary layer. Thus, the generation frequency of the synthetic turbulent boundary layer does not appear, at least in this case, to

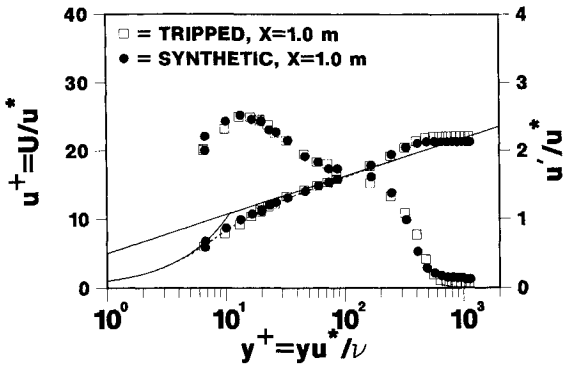

Fig. 11 Inner scaled turbulence intensity and mean velocity profiles.

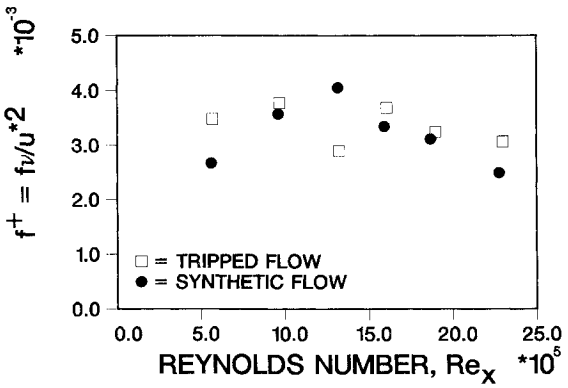

Fig. 12 Boundary-layer burst frequency as a function of X-Reynolds number.

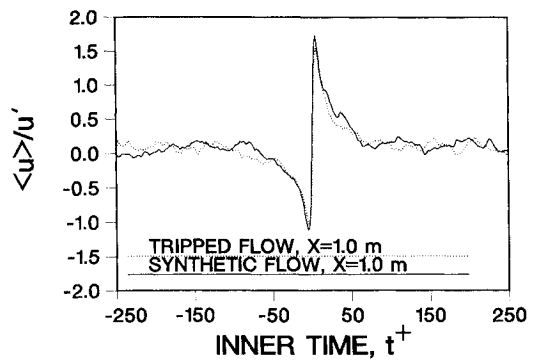

Fig. 13 Conditionally averaged velocity.

control the boundary-layer bursting process as recognized using the VITA technqiue. The VITA conditional averages of the two cases also display close similarity, as may be observed in Fig. 13, which is typical of results throughout the flow. The results are in good agreement with the literature for developed turbulent boundary layers. Thus, from the standpoint of this application of the VITA technique, the synthetic generation of the turbulent boundary layer does not appear to result in alterations in the boundary-layer bursting behavior.

While the mean and turbulence profiles and the VITA bursting frequencies and conditional averages of the two flows are very similar, oscilloscope observations of the hot-wire signal indicated that differences did exist. Remnants of the generation process could be seen in the hot-wire signal near the top of the synthetic boundary layer, most clearly at the more upstream measurement locations. This component of the flow was analyzed with ensemble phase averaging using the jet/spot generation signal as the timing reference. Figure 14 presents

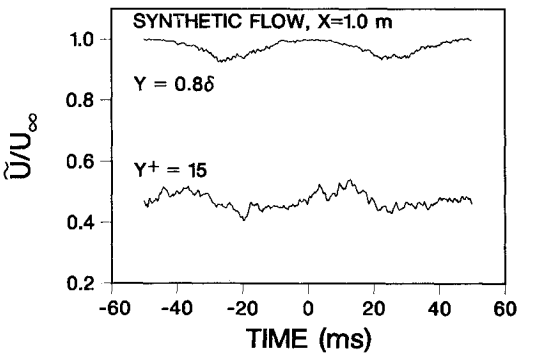

Fig. 14 Synthetic boundary-layer phase-averaged velocities.

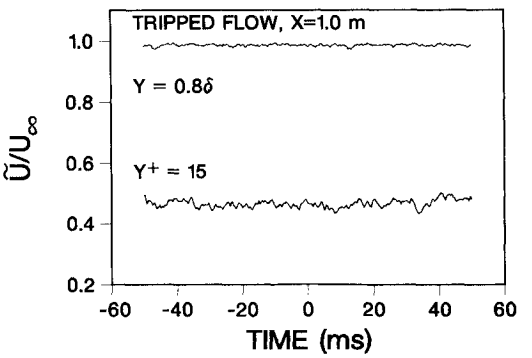

Fig. 15 Tripped boundary-layer phase-averaged velocities.

phase averages of the velocity at $y^+ = 15$ and $y/\delta = 0.8$ for the synthetic boundary layer at $X = 1.0$ m. The evidence of the structures used to generate the boundary layer is quite clear. Measurements indicated that this structure had considerable spanwise uniformity. These phase averages were formed from about 75 realizations. To give an idea of the noise in the averages, the same averaging procedure was applied to the tripped flow, using the same timing reference signal, which in this case had no connection to the flow. The resulting phase averages may be seen in Fig. 15.

The turbulent spots used to generate the synthetic boundary layer were evident in the phase averages measured at $y/\delta = 0.8$ at considerable downstream distances. Near the wall, the phase averages did not show such strong indications of the original pulsating jets. However, the limited number of realizations may have been insufficient to extract the signal from the noise of the higher turbulence levels near the wall.

The phase-averaged results naturally raise the question of whether the signature of the generating spots detected near the top of the boundary layer has any relation to the behavior of the flow nearer to the wall. This problem of the relationship between the outer and inner flows has been addressed in studies of the frequency of occurrence of turbulent boundary-layer bursts and ejections. Researchers have debated whether inner or outer flow parameters can provide proper universal scaling for the bursting frequency; see, for example, Blackwelder and Haritonidis.[9] The clear, though weak, presence of periodic alterations in the outer flow of the synthetic boundary layer thus suggested an attempt to search for a link between these remnants of the generating spots and the bursts detected in the inner flow.

Attempts to find such a link between the VITA detected bursting events and the forcing signal in the synthetic boundary layer suggest that, if it indeed exists, it is quite tenuous. Phase averages formed from a number of parameters revealed very little. Event detection times, the VITA variance, and

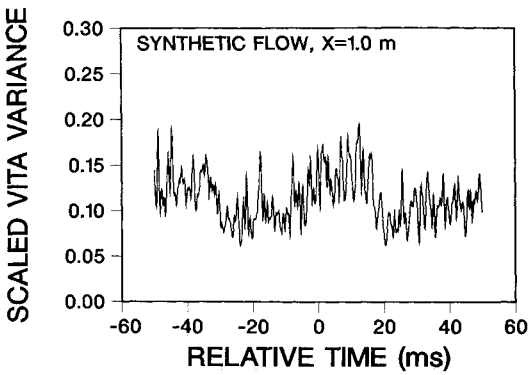

Fig. 16 Synthetic boundary-layer phase-averaged VITA variance.

clipped and scaled versions of the VITA variance were phase averaged, but provided no solid evidence linking the outer flow to the VITA-detected bursts. The phase average of the VITA variance, calculated in the same way as the velocity phase averages, is typical. It is shown in Fig. 16. One may observe a hump, but must note that the magnitude is very low, as a level of 1.0 is required to meet the definition of a detection. A similar dummy phase average calculated for the tripped flow reveals that this structure is a characteristic of the synthetic boundary-layer flow. However, it cannot be said that the phase average does provide convincing evidence of a link between bursting and the boundary-layer generation parameters.

Discussion

The research reported here was conducted in order to answer the questions: could synthetic boundary layers be produced having skin-friction drag less than that of normal turbulent boundary layers over long distances; if the skin-friction drag were reduced, how far downstream did the reduction last; and how did these reductions come about?

The results of the experiment suggest that for the synthetic boundary-layer generation parameter range investigated only very small drag reductions are possible. The development of the synthetic boundary layers was found to be very similar to that of the tripped boundary layer employed as a reference case. The differences in the local skin-friction coefficients appeared to result from shifts in the effective origins of development. It appears that the spots generated to form the synthetic boundary layer interacted in such ways that within perhaps 150 initial boundary-layer thicknesses most of the characteristics of the boundary layers were very similar to those of natural turbulent boundary layers.

These results differ from those of Goodman,[6] who indicates that for his experiment the differences resulted from actual changes in development rather than simple shifts of origin. Goodman's boundary layers were generated using much higher frequencies and somewhat narrower spacings than the present work. His results were limited to the fairly low X-Reynolds number of 5.6×10^5. His paper does not present measurements detailing the changes in development.

The hypothesis for the study was that the artificially generated spots would interact in such ways that the individual spot growth would be reduced and the spatial and temporal scales would be maintained in the resulting synthetic turbulent boundary layer with consequent reductions in skin friction. Coles and Savas[2] observed significant regions of coherent flow in some of their synthetic boundary layers, but did not measure skin friction or flow structure near the wall.

The results of the experiment do suggest that the synthetic boundary layers maintained a certain degree of coherence. The signature of the spot generators used to produce the synthetic turbulent boundary layers was visible very far downstream through the use of the velocity phase averages. At $y/\delta=0.8$, the phase averages exhibited a clear pattern at downstream distances corresponding to at least 300 initial boundary-layer thicknesses.

Additionally, oscilloscope traces of the signal from hot wires near the very top of the synthetic boundary layer showed regions of laminar freestream flow periodically interrupted by regions of turbulence. This pattern exhibited a strong spanwise uniformity and a period that corresponded to each firing of the spot-generating jets. The observations suggest that the many small turbulent spots produced rapidly grew together, forming a peaked turbulent front or wave extending above the nominal boundary-layer thickness.

Thus, in the synthetic boundary layer each turbulent front or "stripe" was followed by a region in which the turbulence did not extend so far above the plate. The next stripe to be observed would then result from the firing of the other half of the spot generators. The firing frequencies employed did not appear to be high enough to cause strong interactions between the spots generated at 180 deg phase lags and the spanwise spacing of the spot generators did not seem to produce a significant spanwise variation in the far downstream flow. This flow may be a more developed version of that which Coles and Savas[2] refer to as the result of their attempt to generate "two-dimensional turbulent spots." The ensemble intermittency measurements of their flow do take the form of turbulent stripes, but spanwise variations are evident.

While the outer region structure exhibits coherence, the result does not suggest that any reduced skin-friction effects might be maintained for very long distances. The pattern resulting from the spot generators seems to be maintained much farther at the very top of the boundary layer than closer to the wall. One might, of course, expect that the remnants of the spots would be maintained longest at the top, where the mean shear and the turbulent mixing are weak. In contrast, the phase-averaged patterns seen at $y^+=15$ decay much more rapidly as a result of the strong turbulent shearing stresses.

The changes in skin-friction drag observed in this experiment and in the previous experiment[5] would seem to result from relatively small differences in the ways in which the synthetically generated flows underwent the transition process between spot generation and development into nominally "regular" turbulent boundary layers. The changes in the effective origins of development of the flows seem to result from this transition or development process. The spots do not act as a sudden trip. Only in this early region of the turbulent flows are dramatic differences observed in the skin-friction coefficients. In the higher Reynolds number regions, the differences between the synthetic flows and the tripped flow become very small. It should be noted that these observations hold only for the limited range of synthetic boundary-layer generation parameters examined.

Conclusions

The conclusions that may be drawn for the synthetic boundary-layer generation parameter range investigated are the following:

1) The mean flow development of synthetic turbulent boundary layers appears to be the same as that of tripped and naturally turbulent boundary layers at sufficient distances downstream of the generation location. In this region, differences in the mean flow parameters can be looked upon as apparent shifts in the origins of development.

2) The synthetic boundary layers do not appear to offer potential for significant skin-friction drag reductions over appreciable downstream distances.

3) While the important mean flow characteristics are little changed in the synthetic boundary layer, the turbulence does differ in reflecting the influence of the generation events.

Acknowledgments

Helpful discussions with A.S.W. Thomas and the aid of W. E. Carter in developing the data acquisition system are gratefully acknowledged. This study was part of an overall program in basic viscous flow research supported by the Lockheed-Georgia Independent Research and Development Program.

References

[1]Coles, D. and Barker, S.J., "Some Remarks on a Synthetic Turbulent Boundary Layer," *Turbulent Mixing in Nonreactive and Reactive Flows*, edited by S.N.B. Murthy, Plenum, New York, 1975, pp. 285-293.

[2]Coles, D. and Savas, O., "Interactions for Regular Patterns of Turbulent Spots in a Laminar Boundary Layer," *Laminar-Turbulent Transition*, edited by R. Eppler and H. Fasel, Springer-Verlag, New York, 1980, pp. 277-287.

[3]Savas, O. and Coles, D., "Coherence Measurements in Synthetic Turbulent Boundary Layers," *Journal of Fluid Machanics*, Vol. 160, 1985, pp. 421-446.

[4]Thomas, A.S.W., personal communication, 1981.

[5]Chambers, F.W., "Preliminary Measurements of a Synthetic Turbulent Boundary Layer," Lockheed-Georgia Co., Marietta, GA, Res. Rept. LG82RR0009, Sept. 1982.

[6]Goodman, W.L., "Emmons Spot Forcing for Turbulent Drag Reduction," *AIAA Journal*, Vol. 23, Jan. 1985, pp. 155-157.

[7]Chambers, F.W. and Thomas, A.S.W., "Turbulent Spots, Wave Packets, and Growth," *The Physics of Fluids*, Vol. 26, 1983, pp. 1160-1162.

[8]Blackwelder, R.F. and Kaplan, R.E., "On the Wall Structure of the Turbulent Boundary Layer," *Journal of Fluid Mechanics*, Vol. 76, 1976, pp. 89-112.

[9]Blackwelder, R.F. and Haritonidis, J.H., "Scaling of the Bursting Frequency in Turbulent Boundary Layers," *Journal of Fluid Mechanics*, Vol. 132, 1983, pp. 87-103.